Volume 3
Number 10
October 2025
Pages 4173–4836

RSC Sustainability

rsc.li/rscsus

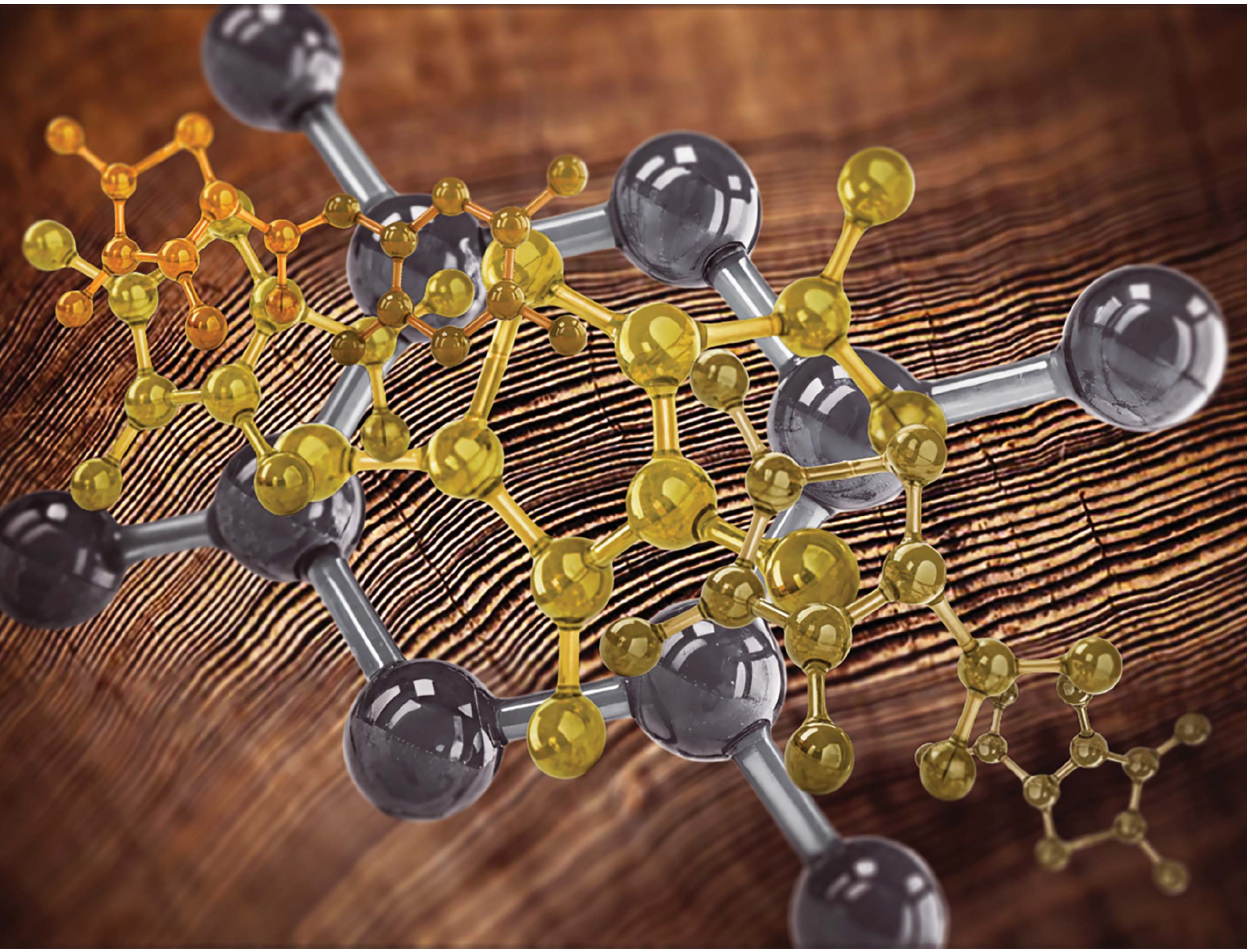

ISSN 2753-8125

ROYAL SOCIETY OF CHEMISTRY

PAPER
Sharib Khan, Sabarathinam Shanmugam, Timo Kikas *et al.*
Lignin depolymerization from softwood biomass using integrated protic ionic liquid–enzyme pretreatment

RSC Sustainability

ROYAL SOCIETY OF CHEMISTRY

PAPER

View Article Online
View Journal | View Issue

Cite this: *RSC Sustainability*, 2025, **3**, 4466

Lignin depolymerization from softwood biomass using integrated protic ionic liquid–enzyme pretreatment†

Sharib Khan, *[a] Daniel Rauber, [b] Luyao Wang,[c] Udayakumar Veerabagu,[a] Christopher W. M. Kay, [bd] Chunlin Xu, [c] Sabarathinam Shanmugam*[a] and Timo Kikas *[a]

Lignin, a vital component of plant biomass, offers significant potential for advanced biorefineries seeking to produce high-value chemicals and materials. However, maximizing lignin yield while ensuring its efficient valorization remains a substantial challenge in biorefineries. In this study, an integrated approach to producing lignin-derived oligomers and monomers was developed from softwood biomass. *Pinus sylvestris* was processed using a protic ionic liquid (PIL), triethylammonium methane sulfonate ([N222H][OMS]), to extract lignin, followed by its targeted depolymerization using bacterial laccases. Advanced analytical techniques were employed to investigate the qualitative and quantitative changes in lignin during the optimization and depolymerization stages. The findings highlight the effectiveness of [N222H][OMS] in removing 87.90% of lignin from pine wood at 180 °C. Furthermore, engineered bacterial laccases demonstrated significant catalytic activity, converting 9.2% of aliphatic hydroxyl groups and 73.8% of phenolic hydroxyl groups in lignin into carboxylic acids. Similarly, benchmarked against commercially available kraft lignin, the same depolymerization approach achieved lower conversion rates, transforming 12.4% aliphatic and 44.5% phenolic hydroxyl groups in lignin into carboxylic acids. Thus, this integrated strategy, combining ionic liquid delignification with enzymatic upgrading, presents a scalable and efficient route for maximizing lignin valorization.

Received 19th May 2025
Accepted 16th June 2025

DOI: 10.1039/d5su00351b

rsc.li/rscsus

Sustainability spotlight

This study introduces a protic ionic liquid, [N222H][OMS], as a sustainable solvent to replace conventional harsh solvents in lignin extraction. Additionally, engineered bacterial enzymes were employed to depolymerize lignin under mild conditions, offering an eco-friendly alternative to traditional chemical and thermal methods. The method collectively advances the sustainability and efficiency of biorefinery operations while aligning with green chemistry objectives. [N222H][OMS] removed 70% of lignin from pine wood biomass at 180 °C. Engineered bacterial laccases selectively depolymerize lignin, converting 9.2% of aliphatic hydroxyl groups and 73.8% of phenolic hydroxyl groups into carboxylic acids. Further studies can focus on reducing the extraction temperature (currently 180 °C) *via* solvent engineering. Also, enzyme immobilization strategies can be developed using closed-loop systems to recover and reuse bacterial laccases, minimizing waste and quantifying environmental impacts to validate and refine the process's green credentials.

1. Introduction

To reduce dependence on finite resources, there is an urgent need to identify bio-based sustainable alternatives that are environmentally friendly and renewable.[1] Among renewable alternatives, lignocellulosic biomass (LCB), which includes agricultural residues, wood, herbaceous plants, *etc.* offers considerable potential as a sustainable resource for producing high-value chemicals and materials.[2,3] Lignin is the most copious biopolymer in LCB after cellulose and is particularly the most promising renewable substitute for petroleum-based materials and chemicals.[4] It is a plant-derived polymer composed of three major building units, p-hydroxyphenyl (H),

[a]*Chair of Biosystems Engineering, Institute of Forestry and Engineering, Estonian University of Life Sciences, Kreutzwaldi 56, 51006, Tartu, Estonia. E-mail: sharib.khan@emu.ee; sabarathinam.shanmugam@emu.ee; timo.kikas@emu.ee*

[b]*Department of Chemistry, Saarland University, Campus B2.2, 66123 Saarbrücken, Germany*

[c]*Laboratory of Natural Materials Technology, Åbo Akademi University, Henrikinkatu 2, Turku, FI-20500, Finland*

[d]*London Centre for Nanotechnology, University College London, 17-19 Gordon Street, London, WC1H 0AH, UK*

† Electronic supplementary information (ESI) available: Detailed experimental method for optimization of lignin depolymerization conditions, figures and tables. See DOI: https://doi.org/10.1039/d5su00351b

guaiacyl (G), and syringyl (S). These units are connected through a range of chemical bonds, including β-O-4, α-O-4, and C–C linkages, which collectively form a complex and resilient structure.[5,6] Although, lignin is an abundant polymer, its structural complexity makes it highly resistant to breakdown, posing a significant challenge for converting lignin into chemicals and materials. Similarly, its inherent recalcitrance and high molecular weight, coupled with contamination from carbohydrates and chemical impurities from the extraction process, pose significant challenges for its valorization, thus resulting in lignin being burned for energy generation rather than used for higher-value applications in pulp industries.[7] To address this, an integrated fractionation technique is essential to valorize lignin, enabling the selective extraction of low-molecular-weight lignin from LCB while efficiently depolymerizing it into monomers or oligomers.[8] Such advancements would also allow pulp industries or biorefineries to maximize lignin utilization in high-value applications, minimize waste, and enhance the overall sustainability of biorefinery processes.[9]

Advanced biorefinery fractionation methods such as reductive catalytic fractionation[2] and aldehyde-assisted biomass fractionation[10] are effective in producing low-molecular-weight lignins from LCB. However, these biomass fractionation methods also face challenges including stringent processing parameters, catalytic fouling and limited lignin yield; therefore effort should be devoted to the search for biobased solvent alternatives that would have significant environmental benefits.[4,9] Ionic liquid (IL) fractionation offers a greener alternative for biomass processing. Among ILs, protic ionic liquids (PILs) are biobased solvents that offer numerous advantages, including low processing temperatures, recyclability, and minimal environmental impact.[11,12] PILs also improve biomass dissolution, enhance cellulose extraction efficiency, and reduce the need for harsh chemicals, contributing to a more environmentally friendly process while producing lower molecular weight lignin fractions. Additionally, PILs facilitate simultaneous lignin modification, such as functional group conversion, which can streamline downstream processing making them a sustainable choice for lignin extraction and LCB fractionation.[13] Still, the integration of lignin depolymerization into PIL-based biomass fractionation remains a significant bottleneck. This requires turning low molecular weight lignin fractions into monomers that can be utilized in higher-value applications, such as cosmetics, drug delivery systems, and coatings.[9] Lignin depolymerization methods, including pyrolysis and base-catalyzed and catalytic depolymerization, are commonly employed to process high molecular weight technical lignins originating from different pulp industries.[3,14,15] Meanwhile, these methods often require substantial energy to break down the complex linkages of lignin, posing challenges, such as high energy consumption and reduced sustainability. In contrast, biological degradation, particularly enzymatic depolymerization, is a greener alternative.[16–18] This approach can convert low-molecular-weight lignin into monomers with lower energy requirements, in alignment with natural processes.

Integrating enzymatic depolymerization with ionic liquid extraction of lignin offers a promising bio-based approach for utilizing LCB. However, some challenges need to be addressed, such as identifying the most suitable enzymes for the process and managing their costs. For instance, laccases (EC 1.10.3.2) are particularly notable for lignin depolymerization, often referred to as "the green enzymes" due to their broad substrate activity and requirement for molecular oxygen as a co-substrate, which results in water as the sole byproduct.[17,19] Furthermore, bacterial laccases have distinct advantages as they show greater tolerance to varying pH levels, solvents, and other demanding conditions, making them particularly well-suited for industrial applications where robust performance is crucial.[16,20–22] Li *et al.* showed that bacterial laccases, exhibit higher catalytic rates than fungal laccases, without the need for redox mediators, effectively depolymerizing lignin or lignin-phenol derivatives.[23] However one of the major shortcomings in using bacterial laccases for lignin depolymerization is their tendency toward strong polymerization activity, which counteracts lignin degradation by re-polymerizing the breakdown products.[24–27] Achieving an effective balance between polymerization and cleavage reactions is therefore essential for promoting biological lignin depolymerization. Thus, optimizing depolymerization conditions, such as redox potential, pH, incubation time, and temperature, can further enhance laccase performance. Additionally, the use of laccase mediators such as 2,2′-azino-bis(3-ethylbenzothiazoline-6-sulfonic acid) in a laccase mediator system (LMS) has been shown to significantly increase laccase activity and broaden the range of oxidized substrates.[28–31] The use of mediators and inconsistent efficiency of laccases, however, add to process costs, thereby affecting economic feasibility. Therefore, the high cost of enzymatic depolymerization remains a substantial barrier to their broader industrial adoption.[18] Advances in genetically engineered bacterial laccases could help overcome these challenges by providing enzymes that are functional, stable under demanding conditions, and do not require mediators.[26,32,33] To date, most studies have focused on the depolymerization of technical lignins, lignin dimers, or lignin in the presence of mediators, with limited investigations into the potential role of ionic liquids in lignin extraction and its integrated depolymerization. Further research is needed to evaluate how ionic liquids can be effectively incorporated into these processes to enhance lignin utilization in biorefineries. Similarly, enzymatic depolymerization and its integration into current PIL based biomass fractionation processes need to be explored. For example, the studies of Peña *et al.*[34] Wufuer *et al.*[35] and Zakaria *et al.*[36] describe the role of ionic liquids in partially depolymerizing lignin during the extraction process.

Building on these considerations, this study presents an integrated approach that combines the ionic liquid pretreatment of softwood biomass with bacterial laccase-mediated lignin depolymerization for the first time. This novel method aims to optimize lignin extraction and depolymerization, thereby enabling the production of low-molecular-weight lignin fractions for high-value applications in a sustainable and economically viable manner.

2. Materials and methods

2.1 Biomass preparation and reagents

Softwood biomass Scots pine (*Pinus sylvestris*) was collected domestically and was de-barked, air-dried to a particle size of 0.5–1 mm, and stored in an airtight container. The moisture content and fiber content of the biomass were measured using a moisture analyzer (MLS-50-3D Kern & Sohn GmbH, Balingen, Germany) and an Ankom 2000 fiber analyzer (ANKOM Technology, USA), respectively. Triethylamine (>99%) and DMSO-d6 (99.9% D) were bought from Sigma-Aldrich (Steinheim, Germany) while methanesulfonic acid (70% aq.) was obtained from Carl Roth (Karlsruhe, Germany); triethylamine was distilled prior to use.

2.2 Synthesis of PIL and its characterization

The PIL triethylammonium methane sulfonate [N222H][OMS] was synthesized by dropwise neutralization of [1.1] equivalents of aqueous triethylamine solution with [1.0] equivalent of aqueous methanesulfonic acid at 0 °C in the laboratory as describe in the previous work.[37] The resulting solution was stirred for 3 h and excess triethylamine and solvent were removed by rotary evaporation and the resulting residue was dried under vacuum at 70 °C for 2 d, yielding the protic ionic liquid in quantitative amounts as a colorless crystalline solid.

2.3 [N222H][OMS]-mediated biomass fractionation

Lignin extraction from pinewood biomass (PWB) using [N222H][OMS] was conducted based on the method described by Khan *et al.*[38] Briefly, biomass and [N222H][OMS] were combined in various ratios (BM/PIL ratios of [1/2], [1/3], and [1/5] w/w%) in a 100 mL ACE pressure tube vortexed and incubated in a preheated oven at varying temperatures (150–210 °C) and incubation times (30–90 minutes). Following pretreatment, ethanol was added to the pressure tube to separate the cellulosic pulp from the [N222H][OMS]–lignin mixture *via* centrifugation (4000 rpm for 10 min). Later, ionic liquid lignin dissolved in ethanol was fractionated using a pressure filtration system equipped with Whatman™ nylon membrane filters (pore size 0.8 μm and diameter 47 mm) to extract lignin rich fractions. Finally, ethanol was recycled using a rotary evaporator (Büchi Rotavapor R-200, Büchi, Switzerland) and after evaporation, water was added to the concentrated ionic liquid solubilized lignin as an antisolvent to precipitate lignin fractions from [N222H][OMS]; the precipitated lignin was subsequently washed (3×) to ensure complete removal of PIL, which was then recovered through centrifugation. An overview of [N222H][OMS] PIL-mediated lignin extraction and enzymatic depolymerization from PWB biomass is presented in Fig. 1. The delignification percentage and lignin yields of PWB using [N222H][OMS] were determined by evaluating the residual lignin in the biomass before and after pretreatment on a dry weight basis. The delignification percentage and lignin recovery were calculated based on the equations describe previously.[38]

2.4 Incubation of lignins with alkaliphilic laccase

The MetZyme® LIGNO™ laccase enzyme suspension obtained from Metgen Oy was centrifuged at 3000 rpm for 10 min (to avoid any interference from residual microorganisms) and the supernatant was used for depolymerization experiments. Laccase activity was determined by estimating the oxidation of 2,2′-azino-bis (3-ethylbenzothiazoline-6-sulfonic acid) at (ε_{436} = 36 000 M^{-1} cm^{-1}) and one unit of enzyme activity was defined as the amount of enzyme that oxidizes 1 μM ABTS per min.[26] Freeze-dried [N222H][OMS] extracted lignin, hereafter referred to as TL, was used for optimizing the depolymerization experiments under different reaction conditions, with a 90 : 10 (v/v) ratio of lignin to enzyme. Prior to the depolymerization experiments, TL was solubilized in 0.1 M NaOH at 1, 5, 10, and 20 g L^{-1} lignin concentrations for 1 h (Fig. 1). Depolymerization experiments were initiated by the addition of laccase enzymes and maintained under constant agitation (150 rpm) at room temperature while control experiments were conducted using heat-inactivated enzymes. After the optimized incubation period, the pH of the mixture was reduced to 2.5 using 3 M H_2SO_4 and the mixture was washed with distilled water (3×) to remove the unreacted residues. The precipitated laccase-treated lignin was obtained through centrifugation (5000 rpm, 10 min, 20 °C) and freeze dried for characterization. Commercially available alkali kraft lignin, hereafter referred to as KL, with low sulfonate content was bought from Sigma-Aldrich, USA.

2.5 Lignin characterization

2.5.1 Gel permeation chromatography. The molecular weight distributions of TL, KL, depolymerized [N222H][OMS]-extracted lignin, hereafter referred to as DTL, and depolymerized alkali kraft lignin, hereafter referred to as DKL were analyzed using a Shimadzu Prominence-i LC-2030C 3D Plus (Shimadzu Corporation, Kyoto, Japan) coupled with gel permeation chromatography (GPC) and LabSolutions GPC software for comprehensive profiling.[38,39] GPC analysis was performed using dual MCX columns with a UV detector, using 0.1 M NaOH as the eluent at an isocratic flow rate of 0.5 mL min^{-1} at 60 °C for 5 mg lignin samples. The relative molecular weights (M_w and M_n) were determined using polystyrene sulfonate sodium salt standards with molecular weights ranging from 1.1 to 100 kDa.

2.5.2 Attenuated total reflection-Fourier transform infrared spectroscopy. The surface functional groups and chemical bonds of different lignin samples were determined using Fourier transform infrared spectroscopy (FTIR) (Spectrum BXII instrument, PerkinElmer Inc., Waltham, MA, USA) with the universal attenuated total reflection (ATR) method in the range of 600–4000 cm^{-1} at a resolution of 4 cm^{-1}.

2.5.3 2-Dimensional-^{1}H–^{13}C heteronuclear single quantum coherence (HSQC) nuclear magnetic resonance (NMR) spectroscopy. The structural linkages in different lignin samples were analyzed using HSQC NMR spectroscopy. Quantitative ^{13}C NMR spectra were obtained on an Ascend Neo 500 MHz spectrometer (Billerica, MA, USA) equipped with a TCI Prodigy cryoprobe in accordance with previously established

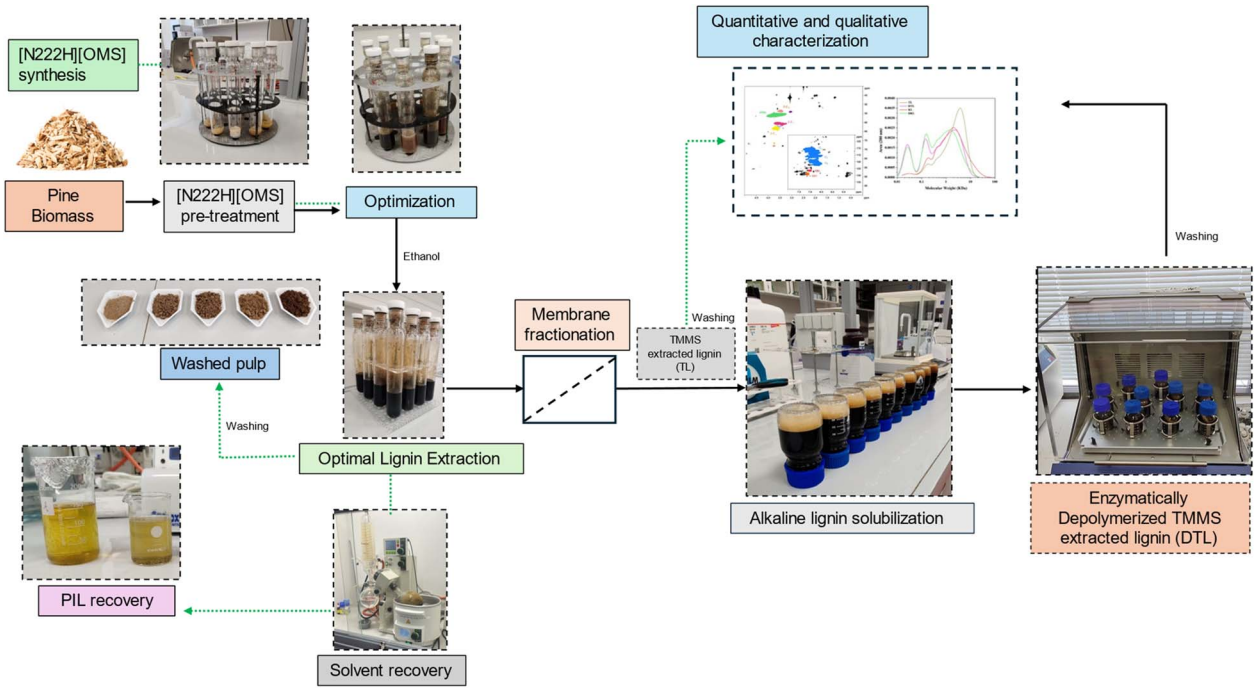

Fig. 1 Overview of the lignin extraction and its depolymerization process from PWB biomass using [N222H][OMS] PIL.

methodologies.[40,41] For the HSQC analysis, lignin (80 mg) was dissolved in deuterated dimethyl sulfoxide (0.5 mL). The experiment was conducted using the Bruker "hsqcetgpsi" pulse sequence with a 2.0 s relaxation delay, an acquisition time of 0.13 s, 256 increments, and 80 scans per increment. The spectral window spanned 8012 Hz (−3.3 to 16 ppm) in the ^{1}H (F_2) dimension and 20 750 Hz (−7.5 to 157.5 ppm) in the ^{13}C (F_1) dimension. HSQC spectra were acquired at 298 K on a Bruker 500 MHz instrument equipped with a smart probe and data processing was performed using Topspin software (version 4.0.6, Bruker).

2.5.4 Quantitative ^{31}P NMR analysis. Quantitative ^{31}P NMR spectroscopy (202.46 MHz, pyridine/$CDCl_3$, 298 K) was used to analyze the distribution of aliphatic hydroxyl (OH), phenolic OH, and carboxylic acid groups in different lignins (TL, KL, DKL and DTL). Approximately 20 mg of freeze dried lignin powder was dissolved in an anhydrous pyridine/$CDCl_3$ mixture (1.6 : 1, v/v) containing Cr(III) acetylacetonate (1.3 μmol) as the relaxation reagent and *endo-N*-hydroxy-5-norbornene-2,3-dicarboximide (12 μmol) as the internal standard, maintaining a lignin-to-standard ratio of 0.6 : 1 (mmol g^{-1}). OH groups were phosphorylated by reacting the solution with 100 μL of 2-chloro-4,4,5,5-tetramethyl-1,3,2-dioxaphospholane for 20 min prior to the ^{31}P NMR measurements.[40,41] Functional group regions in the spectrum were integrated as follows: (a) 150–145 ppm for aliphatic OH, (b) 145–140.8 ppm for syringyl-OH and C_5-condensed-OH, (c) 140.6–138.8 ppm for guaiacyl-OH, (d) 138.6–137.1 ppm for carboxylic acids, and (e) 136–133.6 ppm for other functional groups.

2.5.5 Pyrolysis/gas chromatography-mass spectrometry (Py/GC-MS). Pyrolysis/gas chromatography-mass spectrometry (Py/GC-MS) of lignin samples was conducted using a Pyrola 2000 pyrolyzer coupled to an Agilent 7890 B GC system with an Agilent 5977 B mass selective detector. A ZB-35 GC capillary column (30 m × 0.25 mm ID and 0.25 μm film thickness) was used. Approximately, 100 μg of lignin sample was placed on a platinum filament and pyrolyzed at 650 °C with a residence time of 2 s. The GC injector temperature was set to 280 °C, and the oven temperature was programmed to ramp from 50 °C (held for 0.5 min) to 320 °C (held for 4 min) at a rate of 8 °C min^{-1}. The relative mass spectra were acquired in electron ionization mode at 70 eV, capturing signals in the range of m/z 35 to 700. An updated version of Agilent ChemStation software with mass spectral databases including Wiley 11th, NIST 2012, and a database developed by the Laboratory of Natural Materials Technology (Åbo Akademi University) since 1970 s was utilized for identification of the recorded substances.[42]

2.5.6 Thermogravimetric analysis. The thermal stabilities of the lignins were determined using thermogravimetric analysis (STD-600, TA Instruments). Approximately, 5 mg of predried lignin was used for each TGA, with a temperature range of 0–800 °C at a rate of 10 °C min^{-1} under N_2 (50 mL min^{-1} flow rate).

3. Results and discussion

3.1 Optimization of the lignin extraction process

The yields of lignin extracted from PWB, along with those of cellulose and hemicellulose were determined and later correlated to the composition of untreated biomass (Table S1 – ESI†). The optimization was aimed at maximizing lignin yield with the capability to further depolymerize lignin using bacterial

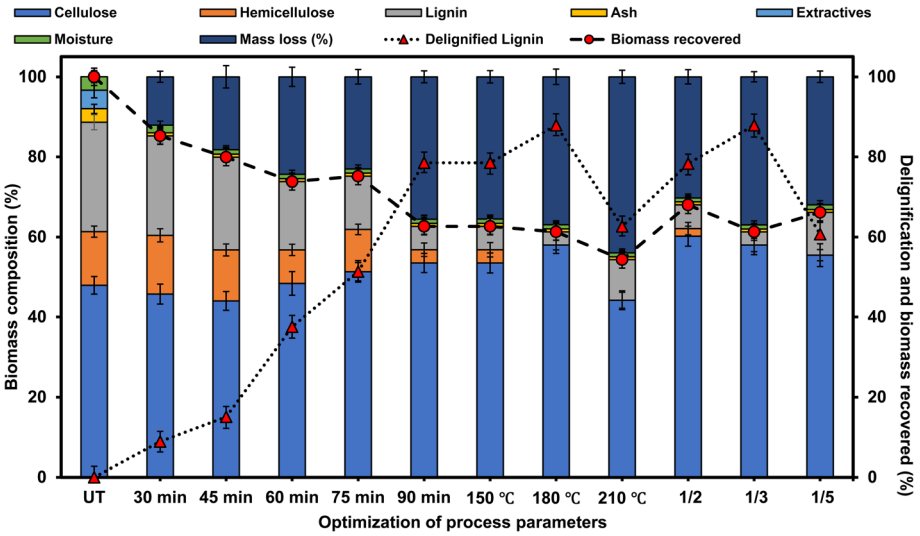

Fig. 2 Optimization of the lignin extraction process from PWB using [N222H][OMs] PIL, focusing on three key parameters: process time, temperature and biomass loading to PIL ratio.

laccases. At first, the effect of incubation time on delignification percentage and lignin yields was studied by varying the incubation time and keeping the other parameters, *i.e.*, the temperature and [BM/PIL] ratio, constant (150 °C with a [BM/PIL] ratio of [1/3]), as shown in Fig. 2. The results suggested that initial incubation time significantly improved lignin and hemicellulose removal. The delignification percentage was found to be significant at 150 °C for 90 minutes, accounting for 78.51% delignification with a biomass recovery of 62.68%. However, after 90 minutes the delignification was gradually reduced. Similar reports by Penín *et al.*,[43] and Gschwend *et al.*[44] describe that PIL-mediated delignification required a prolonged incubation period after which lignin yields decreases significantly. Hence, the optimized [N222H][OMS] pretreatment period of 90 minutes at 150 °C was considered as the efficient delignification and recovery time for lignin extraction from PWB. Next the incubation temperature was studied as it also plays a significant role in delignification and lignin recovery from biomass. Recently, Nurdin *et al.*[45] described that [N222H][OMS] required an optimal incubation temperature of 120 °C for providing good performance in the LCB pretreatment. Thus, the delignification of PWB at three different temperatures (150 °C, 180 °C, and 210 °C) for 90 minutes at a BM/PIL ratio [1/3] was explored. It was found that [N222H][OMS]-mediated delignification and lignin recovery from PWB significantly increase with an increase in temperature. The maximum delignification (87.90%) and lignin extraction (70%) using [N222H][OMS] was achieved at 180 °C. Also, under these optimal process conditions the cellulose percentage of the recovered pulp was about 80% ± 3 while 20% consisted of residual lignin and PIL impurities. This phenomenon is due to the reduced viscosity of [N222H][OMS] at higher temperatures, which further increases the involvement of biomass with the ionic liquid and improves the mass-transfer properties.[46] Additionally, acid attack on the ether linkages by the ammonium proton in [N222H][OMS] is involved in the breakage of the β-O-4′ aryl ether bond, facilitating the simultaneous delignification and depolymerization of lignin.[47,48] However, the delignification yield at 210 °C was reduced significantly to 60%; this effect could describe the increased crystallinity of biomass, where sugars and lignin begin to convert into char while increasing the pre-treatment temperature. Recently, Weerachanchai *et al.*[49] described that LCB pretreatment at higher temperatures showed a sharp decline in regenerated biomass and lignin extraction while giving a higher crystallinity index at pretreatment temperature above 180 °C. Nevertheless, the economic sustainability of ionic liquid-mediated biomass pretreatment predominantly depends on a higher biomass loading ratio as described by Brandt-Talbot *et al.*[13] Thus, biomass fractionation was carried out at 180 °C for 90 minutes at three different biomass loading ratios. From Fig. 2, it is evident that the optimum biomass loading for efficient lignin extraction is a BM/PIL ratio of [1/3] w/w%, which was most effective. Biomass loading ratios of [1/2] and [1/5] also showed similar rates of delignification, possibly because the efficiency of [N222H][OMS] at 180 °C for 90 minutes significantly enhanced the mass transfer properties due to reduced viscosity. However, the improved cellulose content at a biomass loading ratio of [1/2] is probably due to the increased biomass wetting in [N222H][OMS] and the [1/5] ratio showed increased mass loss due to higher acidic attack on the PWB.

3.2 Enzymatic depolymerization of lignins

After optimizing the extraction of lignin from PWB, the dry material was solubilized in a 0.1 M NaOH solution to evaluate various lignin concentrations solubilizing under different alkaline conditions and to identify the optimal parameters for enzymatic depolymerization. High-performance SEC was used to determine the changes in weight-averaged molecular weight (M_w) and number-averaged molecular weight (M_n) of the lignins. The method to calculate the changes in weights was

developed previously and the variations in weights and numbers were used to evaluate the differences in the sizes of different lignin polymers.[39] The optimal temperature for the engineered laccases had been previously established,[26] so determining the ideal lignin concentration, pH and reaction time for TL was essential to maximize the efficiency of depolymerization and ensure accurate characterization. Previously, Liu *et al.*[50] describe a chemoenzymatic approach for lignin depolymerization involving a laccase-catalyzed oxidation reaction at ambient temperature followed by NaOH-induced depolymerization in aqueous solution at 37 °C. To achieve this, we conducted a series of experiments to assess the impact of lignin concentration, pH and reaction time on enzymatic digestion (details can be found in the ESI – Fig. S1, S2 and S3†). The findings revealed that a lignin concentration of 1 g L^{-1} was optimal for achieving maximum depolymerization without significant repolymerization. This was supported by changes in molecular weights and the polydispersity index (PDI), which highlighted a balance between effective depolymerization and minimal repolymerization. The optimal depolymerized lignin molecular weights M_w and M_n values were found to decrease in TL from 3591 to 2044 g mol^{-1} and 1105 to 164 g mol^{-1}, respectively. Similar results were observed using commercially available alkali kraft lignin (KL) and depolymerized kraft lignin (DKL), where the enzymatic depolymerization of KL yielded significant reductions in molecular weights. The M_w of KL (4585 g mol^{-1}) decreased to 1967 g mol^{-1} after treatment, confirming substantial fragmentation of the lignin polymer. Additionally, the polydispersity index (PDI) increased after enzymatic digestion as also shown in Table 1. Similar PDI values were achieved by Prado *et al.*[47] where they performed catalytic oxidative depolymerization of willow biomass subjected to different pretreatment conditions with triethylammonium hydrogen sulfate as the solvent. This rise in PDI suggests heterogeneous cleavage patterns, likely due to variations in lignin subunit reactivity or enzyme accessibility, resulting in a mixture of oligomers and smaller aromatic fragments as shown in the chromatogram (Fig. 3).

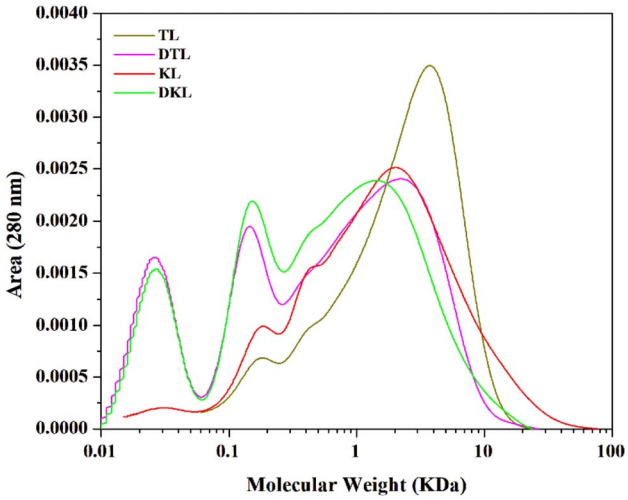

Fig. 3 Size exclusion chromatogram showing reduction in molecular weight profiles of different lignin samples.

3.3 Determining the functional groups of lignins

Significant changes in the intensity of peak bands were observed between 3672 and 3002 cm^{-1}, 2994–2806 cm^{-1}, and 1795–971 cm^{-1} (the lignin fingerprint region) when comparing TL, DTL KL and DKL.[19] These results are consistent with the changes or decreases in the molecular weights observed using HP-SEC. The absorption peak at 3272 cm^{-1} in DTL shows higher intensity and a shift compared to TL, which is attributed to the O–H stretching vibrations of the aliphatic and phenolic hydroxyl groups. These findings are consistent with earlier reports where β-O-4 cleavage leads to an increase in hydroxyl groups and a reduction in C–H stretching vibrations (2994–2806 cm^{-1}).[51] This increase in intensity is due to the higher number of hydroxyl groups present in depolymerized lignin following demethylation.[20,50,52] The lower intensity bands between 2994 and 2806 cm^{-1} in DTL indicate significant C–H stretching vibrations, with a bending vibration at 1453 cm^{-1} associated with methyl and methylene groups.[53] The increased intensity at 1632 and 1509 cm^{-1} in DTL is likely due to the presence of conjugated *p*-substituent carbonyl and carboxyl groups, as well as C=C skeletal vibrations of the benzene ring, respectively.[35] The peak at 1233 cm^{-1} corresponds to C–O stretching vibrations of the syringyl ring, whereas the absorbance peak at 1086 cm^{-1} is attributed to C–O vibrations in secondary alcohols and aliphatic ether linkages.[34,36] By contrasting the ATR FTIR analysis of lignin samples (Fig. 4), it was concluded that the decrease in intensity at different peaks, along with the increased intensity at 1632 and 1509 cm^{-1} in DTL, clearly indicates that the oxidative demethylation of lignin results in the breakdown of the complex lignin structure into smaller fragments of lower molecular weight aromatic compounds.[54]

Table 1 Molecular weights and PDI of TL, DTL, KL and DKL

	M_n	M_w	PDI
TL	1105	3591	3.25
DTL	164	2044	12.46
KL	601	4585	7.63
DKL	173	1967	11.37

3.4 Structural insights and hydroxyl group quantification *via* HSQC and ^{31}P NMR

The aliphatic oxygenated side-chain region (δ_C/δ_H 50–90/3.0–6.0) and the aromatic region (δ_C/δ_H 90–150/6.0–9.0) were analyzed, and peak assignments were made as summarized in the accompanying Table S2 (ESI†). Various interunit linkages and end groups were identified in TL but not in DTL. Similarly, the commercially available KL was compared with DKL that showed similar results where major linkages and groups were unidentified (ESI†). The cross-peaks corresponding to the β-O-4 structure for C_α–H_α, C_β–H_β, and C_γ–H_γ were characterized in TL

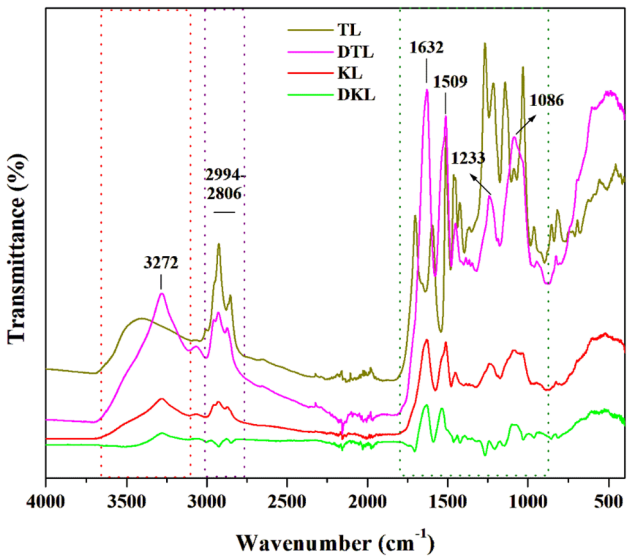

Fig. 4 ATR-FTIR infrared spectra of different lignins indicating the oxidative depolymerization in DTL and DKL.

at δ_C/δ_H 72.1/4.7, 85.2/4.6, and 60.1/3.6/3.2, respectively.[18,24] Additionally, other interunit linkages, such as phenylcoumaran (β-5) at δ_C/δ_H 86.8/5.49 (α), 54.5/3.47 (β), and 63.9/3.73/3.62 (γ); resinol (β–β) at δ_C/δ_H 85.1/4.63 (α), 54.2/3.07 (β), and 70.9/4.16/3.66 (γ); and *trans*-stilbene (SB1) at δ_C/δ_H 125.0/7.01 (α) and SB5 at δ_C/δ_H 128.0/7.12 (α) and 120.0/7.22 (β) were detected in TL but not in DTL.[55–57] Comparing the HSQC spectra between TL and DTL, the absence of cross-peaks in DTL indicates the breakdown of interunit linkages in lignin into uniform monomers, leading to fewer cross-peaks observed in DTL (Fig. 5). Similarly, the disappearance of cross-peaks for β-O-4 linkages (Cα–Hα) at δ_C/δ_H 72.1/4.7 confirms the cleavage of these dominant linkages, which are known to contribute significantly to lignin's structural rigidity. These linkages were not detected in the DTL sample, indicating the successful depolymerization of lignin. Their breakdown suggests the potential for producing smaller, more reactive monomers. Previous studies have also suggested that after depolymerization, the monomer units formed may undergo condensation reactions to produce new C–C bonds, resulting in a reduction of structural heterogeneity and fewer cross-peaks in the HSQC spectrum.[19,21,27,30,58,59] However, the absence of condensed cross-peaks at δ_C/δ_H 67.5/4.21 ppm in the DTL spectrum suggests that such condensation reactions did not occur, further confirming the effective breakdown of lignin interunit linkages.[42,60,61] Nevertheless, TL was extracted from softwood biomass (pine) primarily consisting of guaiacyl (G) units with minor amounts of syringyl (S) units. After enzymatic depolymerization, G units in DTL were evident, with $^{13}C–^{1}H$ correlations at δ_C/δ_H 114.2/6.77 and 115.0/6.68 ppm corresponding to $C_5–H_5$ and $C_6–H_6$, respectively,.[19] The *p*-

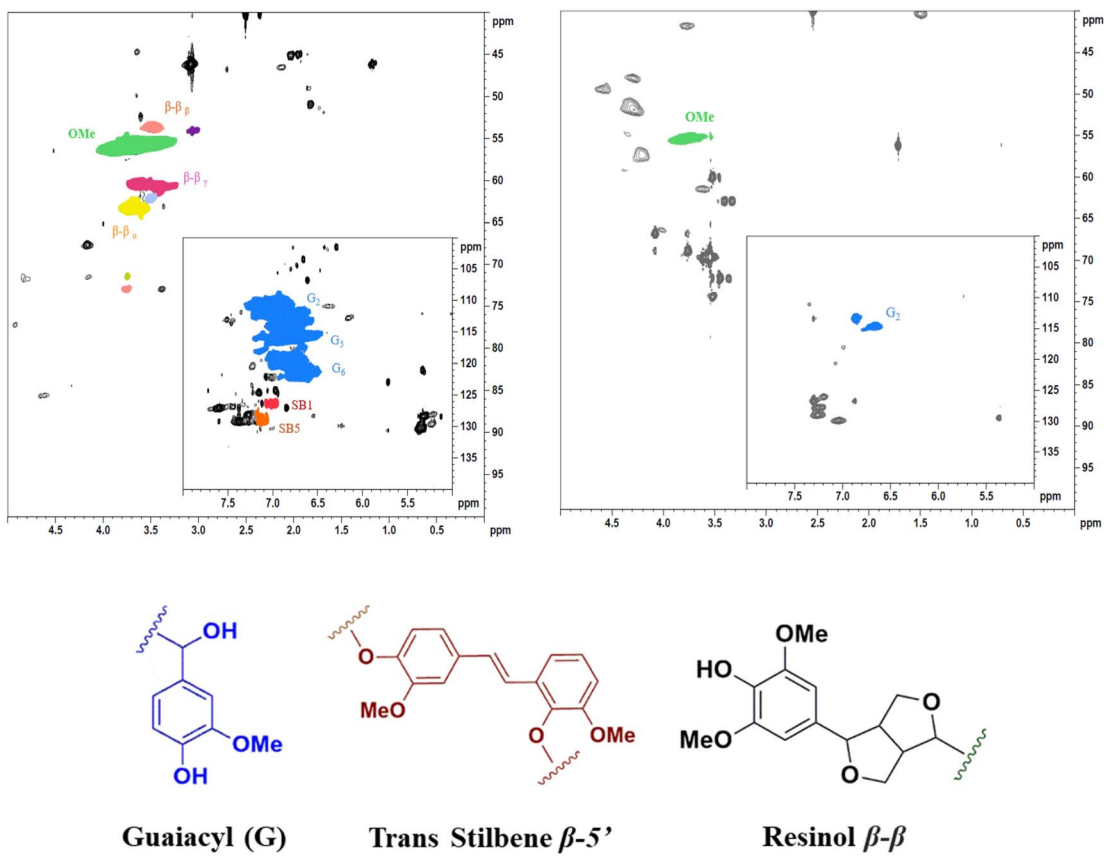

Fig. 5 Major substructures and interunit linkages (aliphatic & aromatic region) absent in depolymerized [N222H][OMS]-extracted lignin (DTL) from pine wood biomass using 2D-HSQC NMR.

Table 2 Presence of aliphatic OH, guaiacyl OH, *p*-hydroxyphenyl OH, and carboxylic acid OH groups in different lignin samples

		Phenolic-OH from lignin					
Samples	Aliphatic- OH[a]	C_5 substituted OH[b]	Guaiacyl-OH[c]	*p*-Hydroxyphenyl-OH[d]	Total phenolic-OH	Carboxylic acid OH[e]	Total OH
TL	1.52	1.09	1.27	0.24	2.60	0.50	4.62
DTL	1.38	0.18	0.23	0.27	0.68	1.37	3.43
KL	2.17	0.73	1.13	0.16	2.02	0.74	4.93
DKL	1.90	0.41	0.33	0.38	1.12	1.67	4.69

[a] Integral of 150–145 ppm. [b] Integral of 145–140.8 ppm; b for both syringyl-OH and C_5-condensed-OH. [c] Integral of 140.6–138.8 ppm. [d] Integral of 138.6–137.1 ppm. [e] Integral of 136–133.6 ppm.

hydroxybenzoate (H) unit signal was observed at δ_C/δ_H 128/7.15 ppm, corresponding to $C_{2/6}$–$H_{2/6}$, although signals for $C_{3/5}$–$H_{3/5}$ and G5 units overlapped.[19,27,30] This suggests that some depolymerized DTL fragments were not fully solubilized in deuterated solvents, an issue previously discussed by many authors.[19,27,30,50] Therefore, the depolymerization of the lignin polymer, which leads to changes in the structure and its properties was difficult to characterize and could explain the weaker signals observed in the HSQC spectrum of DTL (Fig. 5). Thus, to further analyze and quantify insoluble depolymerized polymers, ^{31}P NMR was utilized.

^{31}P NMR is a widely used technique for quantifying the free phenolic and total hydroxyl groups in lignin samples. The results shown in Table 2 suggest a decrease in aliphatic OH, C_5 substituted OH, guaiacyl OH, p-hydroxyphenyl OH groups in DTL and DKL. This shows that phenolic –OH amount in TL (2.60 mg g^{-1}) was higher than that in DTL (0.68 mg g^{-1}) where 9.2% of aliphatic and 73.8% of phenolic hydroxyl groups were converted into carboxylic acids. Similarly, after depolymerization phenolic OH and aliphatic OH amount in KL decreased from 2.02 to 1.12 mg g^{-1} (44.5% conversion) and 2.17 to 1.90 mg g^{-1} (12.4% conversion) into carboxylic acids, signifying oxidative conversion which indicated the depolymerization of TL and KL with the engineered laccases. Di Marino *et al.*[62] recently described an electrochemical process that leads to stable carboxylic acids with high yields of 6.4, 26.8, and 4.2% for oxalic, formic, and acetic acids. While Zhu *et al.*[19] and Zhang *et al.*[63] used bacterial enzymes to provide insights into the depolymerization mechanism of bacterial laccases for lignin, their results similarly demonstrated the degradation of lignin into smaller products. Overall, previous reports reveal that phenolic OH undergo more cleavage with laccases compared to aliphatic; thus, in this study it was also acknowledged that phenolic OH is converted into carboxylic acid while undergoing depolymerization. Vignali *et al.*[52] also proposed that bacterial depolymerization also occurs on aliphatic OH groups which could be present at higher ratios compared to phenolics. Such depolymerization is associated with a significant increase in the extractable monomeric and dimeric compounds, which can arise from etherase activity. Furthermore, quantitative investigations of the low molecular weight compounds using Py-GC/

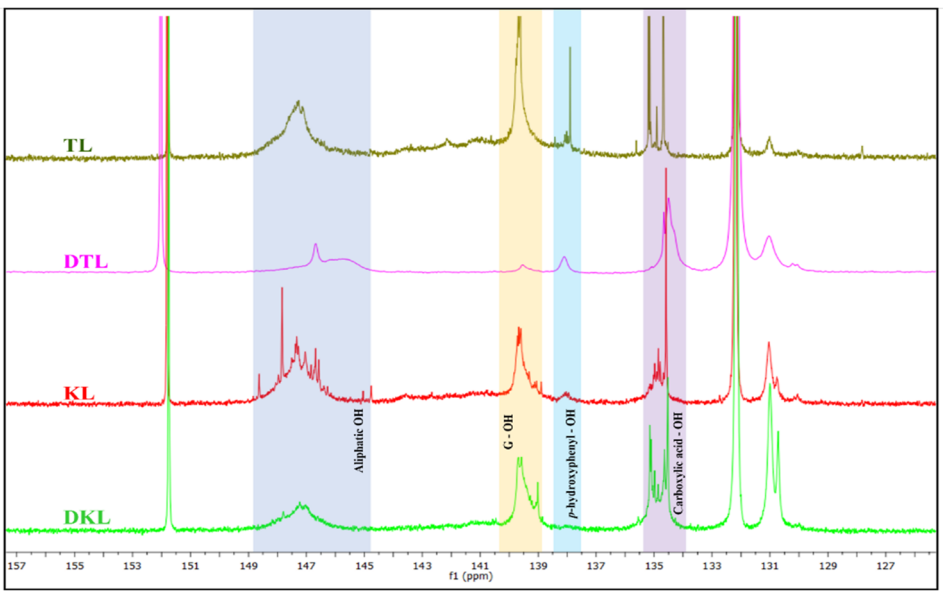

Fig. 6 Comparison of aliphatic OH, guaiacyl OH, *p*-hydroxyphenyl OH, and carboxylic acid OH groups in extracted and depolymerized lignin samples.

MS and thermal gravimetric analysis were performed to understand the underlying reaction (Fig. 6).

3.5 Monomers and oligomers found in different lignins

Recently, Liu *et al.*[41] described a feasible and convenient Py-GC/MS approach for the quantitative investigation for compounds released during pyrolysis that are indicative of substructures present in the lignin polymer. Henceforth, similar Py-GC/MS quantification of TL and KL lignin samples was performed and compared with the depolymerized DTL and DKL to acknowledge the changes occurring in the lignin backbone. The standard mass spectral NIST library was used to assign chromatographic peaks to lignin compounds in the mass spectrometry spectra. The amount of each degradation product was elucidated from the corresponding peak area in the chromatogram of lignins (ESI†). A total of 29 known compounds and 6 unknown compounds were found in TL, with major peak areas corresponding to guaiacol, 4-vinylguaiacol, methyl guaiacol, eugenol, *cis*-isoeugenol, hexadecenoic acid and *cis*-13-octadecenoic acid. Similarly, 39 known compounds and 59 unknown compounds were found in DTL corresponding to the major peak areas of phenol, *o*-creosol, guaiacol, 4-vinylguaiacol, 4-methylguaiacol, *trans*-eugenol, *cis*-isoeugenol, acetovanillone, indole, 4-methyl-1*H*-indole, myristic acid, hexadecenoic acid, dodecanoic acid, oxirane and methyl benzene. All spectra and detailed tables of compounds identified in TL, DTL, KL and DKL are included in the ESI.† The results demonstrated that after depolymerization the number of unidentified compounds increased tremendously in DTL while guaiacyl-type (G) compounds decreased when compared with TL as shown in Fig. 7. Furthermore, laccases can break the linkages between lignin units, as well as cleave branched chains, and generate aromatic compounds and organic acids. Similarly, pyrolysis-GC/MS identified an increase in the number of low-molecular-weight phenolic compounds (*e.g.*, guaiacol and syringol) in depolymerized lignins, which is consistent with the molecular weight reduction. Consequently, these analyses are in good agreement with the HP-SEC, ATR-FTIR, HSQC, and ^{31}P NMR results. In addition, as described by Vignali *et al.*[52] the increase in the peak areas of the small molecules of organic acids can be significantly higher than the increase in the peak area of the aromatic compounds, presumably due to the generation of carboxylic acids through the splitting of the aliphatic side chains and phenolic OH. Similarly, these engineered laccases facilitate side-chain excision and the cleavage of bonds between lignin units.[18,22] Another aspect to consider is that the large number of low-molecular-weight compounds are observed in TL, which could be due to the destruction of the lignin structure during the [N222H][OMS] pre-treatment of softwood biomass.

3.6 Thermal gravimetric analysis (TGA)

The initial weight loss (stage I) for lignin samples was observed between 45 and 200 °C, with weight losses of approximately 3% in TL and 7% in DTL, respectively (Fig. 8). This initial loss was attributed to the evaporation of external water molecules bound to the samples. In the second pyrolysis stage, DTL and DKL exhibited a more significant weight loss and lower thermal stability than TL and KL. Similarly, DTL underwent gradual pyrolysis between 200 °C and 435.5 °C (stage II), resulting in a maximum weight loss rate of 63%. In contrast, TL lost only approximately 39% of its weight in the same temperature range. At temperatures exceeding 450 °C (stage III), DTL experienced a total mass loss of approximately 76%, whereas TL exhibited a lower mass loss of approximately 59%. Greater degradation in DTL results in less solid residue, meaning that fewer unreacted by-products are left behind. This is advantageous for minimizing waste and improving process efficiency. Overall, DTL

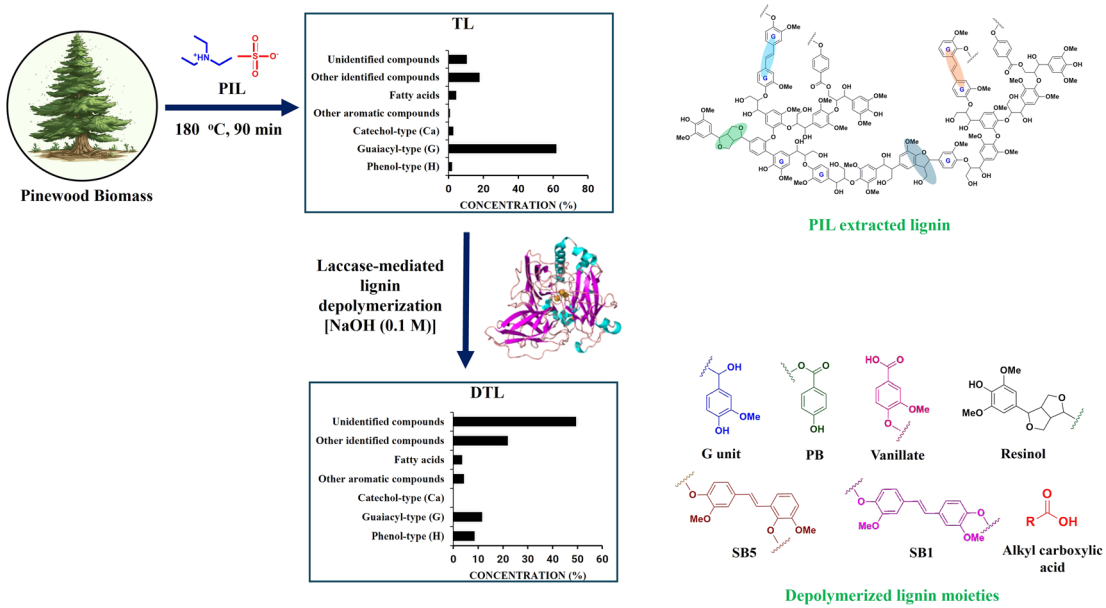

Fig. 7 Quantitative investigations of the low molecular weight compounds characterized in TL and DTL using Py-GC/MS.

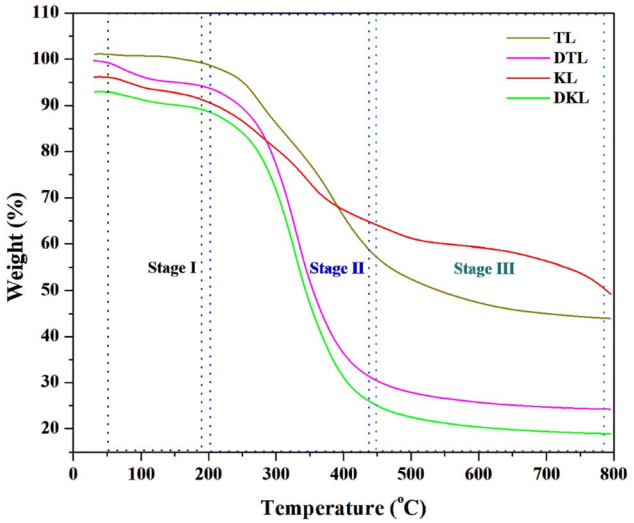

Fig. 8 Thermogravimetric analysis of TL and DTL in three different stages from pine wood biomass.

and DKL showed greater mass loss at high temperatures, indicating its superior performance in thermal degradation processes, with benefits ranging from higher product yields to increased reactivity and environmental efficiency. Furthermore, TL exhibited a higher thermal decomposition temperature (~436 °C) compared to DTL (~375 °C). These differences in the thermal behaviour can be attributed to the distinct chemical structures of different lignins. The higher stability of TL and KL is likely due to their higher molecular weight and the presence of extensive cross-linking between aromatic rings and C–C linkages.[64,65] Conversely, the lower stability of DTL and DKL is associated with their lower molecular weight and the presence of more uniform monomers, such as phenolic compounds, as well as aliphatic and carboxylic acid OH end groups. Based on the TGA analysis, it is evident that depolymerized lignins that have lower molecular weights produce more volatile compounds, as indicated by their lower decomposition temperature (~375 °C) and greater overall weight loss (~76%).

4. Conclusion

Herein, an integrated approach for lignin extraction and subsequent depolymerization was presented. The findings reveal that PIL pretreatment of LCB combined with laccases oxidize both aliphatic and phenolic groups in lignin, generating phenoxy radicals. These radicals destabilize the lignin polymer, promoting the cleavage of aryl-ether linkages (such as β-O-4) and minor C–C bonds. This oxidative cleavage ultimately results in the breakdown of lignin into smaller aromatic molecules and carboxylic acids. The factor, which played an important role, was the use of PIL-extracted lignin with a lower molecular weight. Furthermore, the dissolution of lignin in aqueous alkaline solution was assumed to be the key to unfolding lignin depolymerization using a biocatalyst. However, as the pH decreases, association processes begin to operate *via* non-bonding orbital interactions with the formation of aggregates and fractals. Therefore, the most important implication of this process is the need to optimize lignin extraction to obtain lower-molecular weights lignin fractions with desired characteristics in terms of molecular weight distribution and functional group content. Altogether depolymerized lignin fractions are associated with a high content of carboxylic acids. Recognizing the potential of depolymerized lignin in the development of high-value bio-based products, future LCB pretreatment strategies could integrate lignin depolymerization into biorefinery processes to support sustainable development.

Data availability

The data supporting this article have been included as part of the ESI.†

Author contributions

S. K. carried out the investigation, experiments, and data analysis as well as wrote the original draft. D. R. L. W. and U. V. assisted in the NMR, Py-GC/MS and TGA analysis. D. R. and S. S. assisted in the PIL synthesis. T. K. and S. S. supervised and conceptualized this study. C. K. and C. X. co-supervised the work. T. K. S. S. and U. V. read through and commented on the manuscript.

Conflicts of interest

The authors declare that they have no conflict of interest.

Acknowledgements

This work was supported by the Estonian Research Council Grant PRG2730 and the EEA Grant of Iceland, Liechtenstein, and Norway (Agreement No. EEZ/BPP/VIAA/2021/7). S. K. would like to acknowledge the Erasmus+ mobility grant "Co-funded by the Erasmus+ Programme of the European Union" and S. S. would also like to acknowledge the Short-Term Scientific Mission (STSM) grant funded by the COST Action (E-COST-GRANT-CA17128-6ca97f20). The authors would like to acknowledge the team at the NMR Service Center at Saaraland University for their support in instrumentation and technical assistance for NMR. They also thank Antoine Mialon (Neste), Petri Ihalainen (VTT), and Anu Suonpää (MetGen) for their valuable discussions about lignin depolymerization and MetGen Oy for sending commercially available and lab-engineered laccases as a gift.

References

1 R. Meys, A. Kätelhön, M. Bachmann, B. Winter, C. Zibunas, S. Suh and A. Bardow, *Science*, 2021, **374**, 71–76.
2 Y. Liao, S.-F. Koelewijn, G. Van den Bossche, J. Van Aelst, S. Van den Bosch, T. Renders, K. Navare, T. Nicolaï, K. Van Aelst and M. Maesen, *Science*, 2020, **367**, 1385–1390.

3 A. J. Ragauskas, G. T. Beckham, M. J. Biddy, R. Chandra, F. Chen, M. F. Davis, B. H. Davison, R. A. Dixon, P. Gilna and M. Keller, *Science*, 2014, **344**, 1246843.
4 M. Y. Balakshin, E. A. Capanema, I. Sulaeva, P. Schlee, Z. Huang, M. Feng, M. Borghei, O. J. Rojas, A. Potthast and T. Rosenau, *ChemSusChem*, 2021, **14**, 1016–1036.
5 M. Y. Balakshin and E. A. Capanema, *RSC Adv.*, 2015, **5**, 87187–87199.
6 R. Vanholme, B. Demedts, K. Morreel, J. Ralph and W. Boerjan, *Plant Physiol.*, 2010, **153**, 895–905.
7 A. Kalliola, P. Kangas, I. Winberg, T. Vehmas, H. Kyllönen, J. Heikkinen, O. Poukka, K. Kemppainen, P. Sjögård and L. Pehu-Lehtonen, *Nord. Pulp Pap. Res. J.*, 2022, **37**, 394–404.
8 W. Schutyser, T. Renders, S. Van den Bosch, S.-F. Koelewijn, G. Beckham and B. F. Sels, *Chem. Soc. Rev.*, 2018, **47**, 852–908.
9 Z. Sun, B. Fridrich, A. De Santi, S. Elangovan and K. Barta, *Chem. Rev.*, 2018, **118**, 614–678.
10 L. Shuai, M. T. Amiri, Y. M. Questell-Santiago, F. Héroguel, Y. Li, H. Kim, R. Meilan, C. Chapple, J. Ralph and J. S. Luterbacher, *Science*, 2016, **354**, 329–333.
11 F. J. Gschwend, F. Malaret, S. Shinde, A. Brandt-Talbot and J. P. Hallett, *Green Chem.*, 2018, **20**, 3486–3498.
12 P. Nakasu, T. Pin, J. Hallett, S. Rabelo and A. Costa, *Renewable Energy*, 2021, **172**, 816–828.
13 A. Brandt-Talbot, F. J. Gschwend, P. S. Fennell, T. M. Lammens, B. Tan, J. Weale and J. P. Hallett, *Green Chem.*, 2017, **19**, 3078–3102.
14 M. Wang and F. Wang, *Adv. Mater.*, 2019, **31**, 1901866.
15 K. Stärk, N. Taccardi, A. Bösmann and P. Wasserscheid, *ChemSusChem*, 2010, **3**, 719–723.
16 C. Chio, M. Sain and W. Qin, *Renewable Sustainable Energy Rev.*, 2019, **107**, 232–249.
17 Z.-B. Guan, Q. Luo, H.-R. Wang, Y. Chen and X.-R. Liao, *Cell. Mol. Life Sci.*, 2018, **75**, 3569–3592.
18 J. C. Chan, M. Paice and X. Zhang, *ChemCatChem*, 2020, **12**, 401–425.
19 D. Zhu, N. Liang, R. Zhang, F. Ahmad, W. Zhang, B. Yang, J. Wu, A. Geng, M. Gabriel and J. Sun, *ACS Sustain. Chem. Eng.*, 2020, **8**, 12920–12933.
20 F. C. Claro, G. G. de Lima, T. A. de Lima, F. A. Hansel, M. Matos, F. Avelino, D. R. Oliveira, D. Lomonaco and W. L. Magalhães, *Biomass Convers. Biorefin.*, 2025, **15**, 2479–2494.
21 D. Rodríguez-Escribano, F. de Salas, R. Pliego, G. Marques, T. Levée, A. Suonpää, A. Gutiérrez, Á. T. Martínez, P. Ihalainen and J. Rencoret, *Polymers*, 2023, **15**, 4433.
22 A. D. Moreno, D. Ibarra, M. E. Eugenio and E. Tomás-Pejó, *J. Chem. Technol. Biotechnol.*, 2020, **95**, 481–494.
23 J. Li, Z. Liu, J. Zhao, G. Wang and T. Xie, *Int. J. Biol. Macromol.*, 2024, **256**, 128487.
24 S. Majumdar, T. Lukk, J. O. Solbiati, S. Bauer, S. K. Nair, J. E. Cronan and J. A. Gerlt, *Biochemistry*, 2014, **53**, 4047–4058.
25 M.-L. Mattinen, T. Suortti, R. Gosselink, D. S. Argyropoulos, D. Evtuguin, A. Suurnäkki, E. de Jong and T. Tamminen, *BioResources*, 2008, **3**, 549–565.
26 V. Hämäläinen, T. Grönroos, A. Suonpää, M. W. Heikkilä, B. Romein, P. Ihalainen, S. Malandra and K. R. Birikh, *Front. Bioeng. Biotechnol.*, 2018, **6**, 20.
27 L. Wang, L. Tan, L. Hu, X. Wang, R. Koppolu, T. Tirri, B. van Bochove, P. Ihalainen, L. S. Seleenmary Sobhanadhas and J. V. Seppälä, *ACS Sustain. Chem. Eng.*, 2021, **9**, 8770–8782.
28 R. Hilgers, J.-P. Vincken, H. Gruppen and M. A. Kabel, *ACS Sustainable Chem. Eng.*, 2018, **6**, 2037–2046.
29 L. P. Christopher, B. Yao and Y. Ji, *Front. Energy Res.*, 2014, **2**, 12.
30 S. A. Mayr, S. Wagner, R. Nagl, A. Pellis, M. Gigli, C. Crestini, M. Horvat, T. Zeiner, G. M. Guebitz and R. Weiss, *ACS Sustain. Chem. Eng.*, 2023, **11**, 17739–17751.
31 J. Dillies, C. Vivien, M. Chevalier, A. Rulence, G. Châtaigné, C. Flahaut, V. Senez and R. Froidevaux, *Biotechnol. Appl. Biochem.*, 2020, **67**, 774–782.
32 O. B. Chukwuma, M. Rafatullah, H. A. Tajarudin and N. Ismail, *Sustainability*, 2020, **12**, 7282.
33 J. F. Osma, J. L. Toca-Herrera and S. Rodríguez-Couto, *J. Environ. Manage.*, 2011, **92**, 2907–2912.
34 C. A. Peña, L. F. Ballesteros, H. Rodríguez, E. Rodil, J. A. Teixeira and M. Michelin, *Biomass Bioenergy*, 2023, **177**, 106928.
35 A. Wufuer, Y. Wang and L. Dai, *Biomass Convers. Biorefin.*, 2021, 1–10.
36 S. M. Zakaria, A. Idris, K. Chandrasekaram and Y. Alias, *Ind. Crops Prod.*, 2020, **157**, 112885.
37 T. K. Dier, D. Rauber, D. Durneata, R. Hempelmann and D. A. Volmer, *Sci. Rep.*, 2017, **7**, 5041.
38 S. Khan, D. Rauber, S. Shanmugam, C. W. Kay, A. Konist and T. Kikas, *Polymers*, 2022, **14**, 4637.
39 S. Khan, K. K. Puss, T. Lukk, M. Loog, T. Kikas and S. Salmar, *Energies*, 2022, **16**, 370.
40 R. Liu, A. Smeds, T. Tirri, H. Zhang, S. Willfor and C. Xu, *ACS Sustain. Chem. Eng.*, 2022, **10**, 14588–14599.
41 R. Liu, A. Smeds, L. Wang, A. Pranovich, J. Hemming, S. Willfor, H. Zhang and C. Xu, *ACS Sustain. Chem. Eng.*, 2021, **9**, 13862–13873.
42 R. Liu, A. Smeds, S. Willför and C. Xu, *Ind. Crops Prod.*, 2024, **209**, 118055.
43 L. Penín, S. Peleteiro, S. Rivas, V. Santos and J. C. Parajó, *BioResources*, 2019, **14**, 4733–4747.
44 F. J. Gschwend, C. L. Chambon, M. Biedka, A. Brandt-Talbot, P. S. Fennell and J. P. Hallett, *Green Chem.*, 2019, **21**, 692–703.
45 M. Nurdin, H. Abimanyu, A. Haris, M. Maulidiyah, M. A. Fitriady, D. Mansur, Z. Arham, D. Wibowo and L. O. A. Salim, *J. Oleo Sci.*, 2021, **70**, 1509–1515.
46 C. L. Chambon, V. Fitriyanti, P. Verdia, S. M. Yang, S. Herou, M.-M. Titirici, A. Brandt-Talbot, P. S. Fennell and J. P. Hallett, *ACS Sustain. Chem. Eng.*, 2020, **8**, 3751–3761.
47 R. Prado, X. Erdocia, G. F. De Gregorio, J. Labidi and T. Welton, *ACS Sustain. Chem. Eng.*, 2016, **4**, 5277–5288.
48 G. F. De Gregorio, R. Prado, C. Vriamont, X. Erdocia, J. Labidi, J. P. Hallett and T. Welton, *ACS Sustain. Chem. Eng.*, 2016, **4**, 6031–6036.

49 P. Weerachanchai, S. S. J. Leong, M. W. Chang, C. B. Ching and J.-M. Lee, *Bioresour. Technol.*, 2012, **111**, 453–459.
50 H. Liu, L. Zhu, A.-M. Wallraf, C. Räuber, P. M. Grande, N. Anders, C. Gertler, B. Werner, J. r. Klankermayer and W. Leitner, *ACS Sustain. Chem. Eng.*, 2019, **7**, 11150–11156.
51 Z. Zhang, R. Yang, W. Gao and X. Yao, *RSC Adv.*, 2017, **7**, 31009–31017.
52 E. Vignali, M. Gigli, S. Cailotto, L. Pollegioni, E. Rosini and C. Crestini, *ChemSusChem*, 2022, **15**, e202201147.
53 M. N. M. Ibrahim, A. Iqbal, C. C. Shen, S. A. Bhawani and F. Adam, *BMC Chem.*, 2019, **13**, 1–14.
54 M. Arefmanesh, T. V. Vuong, S. Nikafshar, H. Wallmo, M. Nejad and E. R. Master, *Appl. Microbiol. Biotechnol.*, 2022, **106**, 2969–2979.
55 C. Zhao, S. Li, H. Zhang, F. Yue and F. Lu, *Int. J. Biol. Macromol.*, 2020, **152**, 411–417.
56 M. E. Eugenio, R. Martín-Sampedro, J. I. Santos, B. Wicklein, J. A. Martín and D. Ibarra, *Int. J. Biol. Macromol.*, 2021, **181**, 99–111.
57 T.-Q. Yuan, S.-N. Sun, F. Xu and R.-C. Sun, *J. Agric. Food Chem.*, 2011, **59**, 10604–10614.
58 A. T. Smit, T. Dezaire, L. A. Riddell and P. C. Bruijnincx, *ACS Sustain. Chem. Eng.*, 2023, **11**, 6070–6080.
59 E. Liu, F. Segato, R. A. Prade and M. R. Wilkins, *Bioresour. Technol.*, 2021, **338**, 125564.
60 M. Karlsson, J. Romson, T. Elder, Å. Emmer and M. Lawoko, *Biomacromolecules*, 2023, **24**, 2314–2326.
61 N. Giummarella, I. V. Pylypchuk, O. Sevastyanova and M. Lawoko, *ACS Sustain. Chem. Eng.*, 2020, **8**, 10983–10994.
62 D. Di Marino, T. Jestel, C. Marks, J. Viell, M. Blindert, S. M. Kriescher, A. C. Spiess and M. Wessling, *ChemElectroChem*, 2019, **6**, 1434–1442.
63 S. Zhang, J. Xiao, G. Wang and G. Chen, *Bioresour. Technol.*, 2020, **304**, 122975.
64 M. Wądrzyk, R. Janus, M. Lewandowski and A. Magdziarz, *Renewable Energy*, 2021, **177**, 942–952.
65 W. Yang, F. Yang, X. Zhang, P. Zhu, H. Peng, Z. Chen, L. Che, S. Zhu and S. Wu, *Biomass Conversion and Biorefinery*, 2021, 1–10.